Vol. 25 • No. 41 • November 6 • 2013

D10488

www.advmat.de

ADVANCED MATERIALS

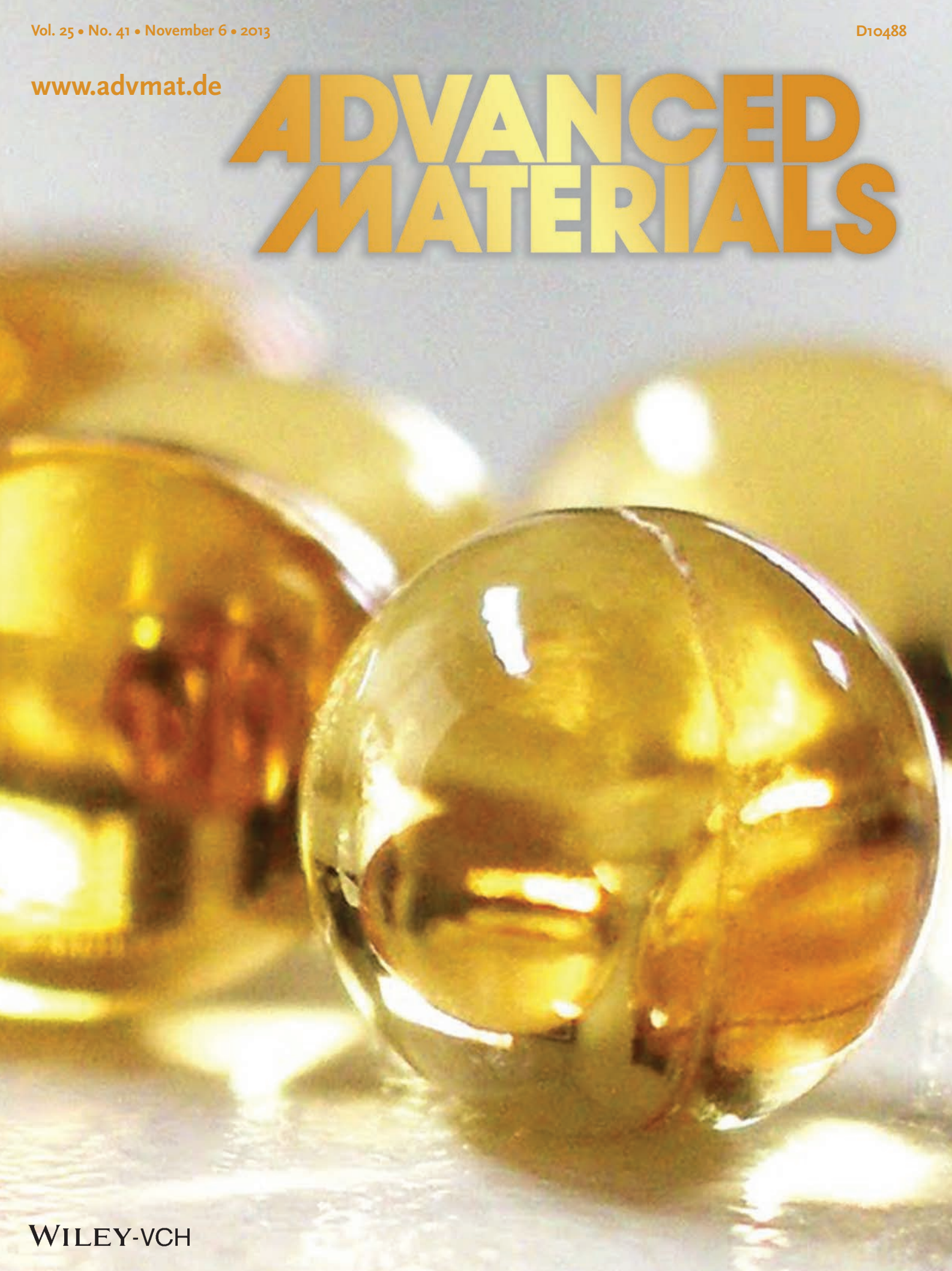

WILEY-VCH

All-Biomaterial Laser Using Vitamin and Biopolymers

*Sedat Nizamoglu, Malte C. Gather, and Seok Hyun Yun**

Laser-based photonic technologies are widely used in medical applications for sensing and diagnosis. Traditionally, optical medical devices are based on solid-state materials, such as glasses and plastics, which have excellent optical characteristics but offer poor biocompatibility. Soft and polymeric biomaterials with desired optical properties and structures have the potential for creating advanced functional devices.[1–6] Such devices may be implanted, integrated into tissues, and even resorbed after use.[7,8] While biopolymers have been used for passive waveguides and as substrates for light-emitting diodes, active photonic devices based on biomaterials remain largely unexplored.[9–11] As an active photonic device, lasers are composed of a pumped gain medium placed within an optical resonator. Conventional gain materials include semiconductors, crystals, and laser dyes. Recently, we have shown that fluorescent proteins are attractive, biologically producible gain materials.[12,13] Using mammalian cells engineered to express green fluorescent protein (GFP) and placing them between a pair of dielectric mirrors, biological cell lasers have been demonstrated. Although fluorescent proteins are promising gain materials, they are not naturally present in the human body and may in fact be immunogenic to some extent. Furthermore, to make the entire laser truly biocompatible, the bulk dielectric mirrors will have to be replaced.

In this communication, we demonstrate a miniature laser based on biomaterials known as Generally-Recognized-As-Safe (GRAS) substances approved by the U.S. Food and Drug Administration (FDA). For the gain medium, we use flavin mononucleotide, a biomolecule produced from vitamin B2, in glycerol-mixed microspheres. Vitamin microspheres with diameters of 10–40 μm were formed by spraying in situ and encapsulated in patterned super-hydrophobic poly-L-lactic acid (PLLA) films. The spheres support lasing at optical pump energies as low as 15 nJ per pulse (≈1 kW mm^{-2}).

Many biomolecules in the human body are known to produce fluorescence upon optical excitation and therefore can potentially be used as a laser gain medium (see Table S1, Supporting Information). However, most of these offer low quantum yields and need to be excited in the biologically harmful ultraviolet (UV) range. Searching through the Database of Select Committee on GRAS Substances, we have identified vitamin B2 (riboflavin) in the form of flavin mononucleotide (FMN) (**Figure 1**a) as a potential laser gain material that is compatible with the human body.[14] FMN serves as coenzyme in a series of oxidation–reduction catalysts and is found in many types of human tissue including heart, liver, and kidney tissue. The molecular structure of FMN forms a quasi-four-level system (Figure 1b). Upon optical excitation to upper states (S1 or S2), the molecule rapidly relaxes to the bottom of the first-excited singlet state (S1) within picoseconds via nonradiative vibrational relaxation and then relaxes back to the ground state (S0) by emitting a photon via fluorescence on a timescale of ≈5 ns or non-radiative rapid internal conversion including transition to the triplet state (T1).[15] The probability of emitting fluorescence is defined as quantum yield. FMN has a relatively high quantum yield of 0.23.[16] Figure 1c shows the typical absorption and emission spectra of FMN. FMN has an absorption cross section of about 2×10^{-16} cm^2 in the visible part of the spectrum and can thus be efficiently pumped in cyan-blue color region (S0->S1).[17]

Lasing occurs in a cavity by stimulated emission (S1->S0), which provides optical amplification. To test the feasibility of the FMN biomolecule as an optical gain medium, we placed aqueous vitamin solution (concentration ≈10 mM) between a Fabry-Perot resonator formed by two identical planar dielectric mirrors (Figure 1d and Figure S1, Supporting Information). The mirrors had high reflectivity (>99.5%) in a spectral range from 490 to 578 nm (Inset of Figure 1d), which covers the emission band of FMN, and low reflectivity (<10%) below 470 nm, which allows the pump light to pass through. The distance between the mirrors was adjusted to ≈23 μm using microbeads.

Figure 1e shows the energy of the output pulses emitted from the resonator as a function of pump energy. We observe a distinct threshold of lasing at a pump energy of 134 nJ, i.e., the output energy increases sharply with the pump energy above this pump level. Below the threshold, the emission spectrum corresponds to the broad spontaneous emission of FMN modulated by the transmission characteristics of the cavity (Figure S2). As the pump energy increases above the threshold, the emission spectrum is dominated by a few distinct spectral lines, which correspond to different longitudinal laser modes (see the inset of Figure 1e). The longitudinal modes have a wavelength spacing of about 5.2 nm, corresponding to the mirror spacing (assuming a refractive index of 1.33 for the FMN solution). We found 10 mM to be the optimal concentration in terms of lasing threshold (Figure 1f). For higher concentrations, non-excited molecules contribute to ground state absorption of the light circulating in the cavity. This generates additional

Dr. S. Nizamoglu, Prof. M. C. Gather, Prof. S. H. Yun
Harvard Medical School and Wellman
Center for Photomedicine
Massachusetts General Hospital
65 Landsdowne St, UP-5, Cambridge
Massachusetts, 02139, USA
E-mail: syun@hms.harvard.edu
Prof. S. H. Yun
WCU Graduate School of Nanoscience and Technology
Korea Advanced Institute of Science and Technology
Daejeon, Korea
Prof. M. C. Gather
Institut für Angewandte Photophysik
Technische Universität Dresden
George-Bähr-Str. 1, 01062, Dresden, Germany

DOI: 10.1002/adma201300818

ADVANCED MATERIALS
www.advmat.de
www.MaterialsViews.com

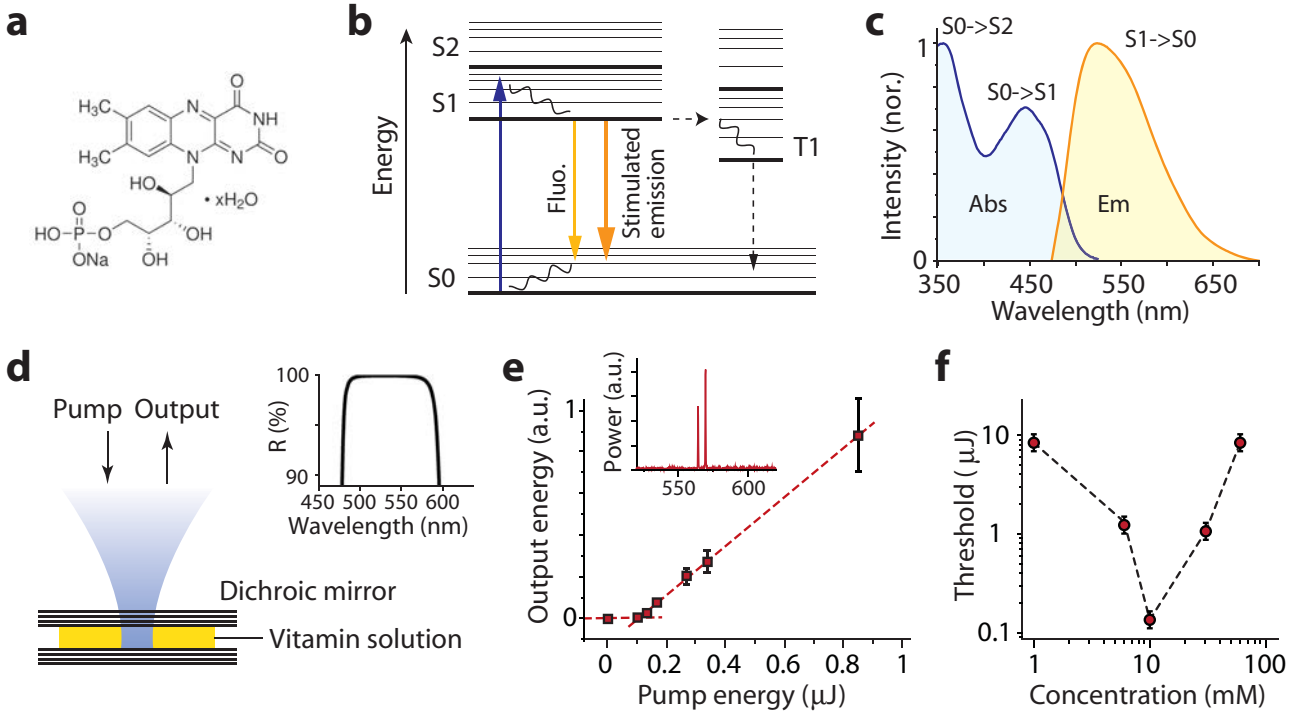

Figure 1. (a) The chemical structure of flavin mononucleotide, riboflavin 5′-monophosphate sodium salt hydrate (also known as FMN-Na). (b) Schematic energy level diagram of FMN and electronic transitions corresponding to optical excitation (S0->S1), spontaneous fluorescence emission and stimulated emission (S1->S0). (c) Measured absorption and emission spectra (10 μM solution). (d) Schematic of the vitamin solution laser. Inset, the measured reflectivity profile of the cavity mirror. (e) Laser output energy as a function of pump energy (per pulse). Lines, linear fits to the data below and above threshold (E_{th} = 134 nJ), respectively. Error bars represent the measurement uncertainty including pulse-to-pulse variation. The inset shows a normalized laser spectrum at a pump energy of 1 μJ. (f) Lasing threshold at various vitamin concentration levels.

optical loss for amplified stimulated emission and increases the threshold. We also tested aqueous solutions of riboflavin and observed similar lasing thresholds. Compared to FMN, however, riboflavin was found to have a lower photo-stability due to its faster transition to non-fluorescent products.[16]

Having confirmed that FMN is a viable gain medium, we sought to replace the bulky dielectric resonator by a biomaterial-based resonator. Aqueous microdroplets can be formed on the superhydrophobic surface of a substrate and can support whispering gallery resonance modes by total internal reflection from the interface between the droplet and the surrounding air[18–20] (Figure S3 for illustration). As for the substrate, there are several natural or synthetic biomaterial options, such as silk,[21] collagen, and polyglycolic acids, which cover a wide range of biodegradation lifetime from hours to years. However, the vast majority of biopolymers do not possess a sufficient hydrophobicity to enable the formation of micro-droplets with large enough contact angles to support low-loss whispering gallery modes (WGM). In this work, we used a synthetic biopolymer of polylactic acid (PLLA), which is approved by FDA for human clinical and ecological applications.[22] We fabricated transparent amorphous PLLA films by heating and pressing. The water contact angle on such flat PLLA film was found to be 67°. To increase the hydrophobicity of the PLLA surface, we developed a two-step procedure consisting of laser micromachining and molding to introduce a defined level of superhydrophobicity to the biofilm (see Methods). A surface-treated polydimethylsiloxane (PDMS) mold was used. Afterward, whispering gallery mode micrdroplet lasers are generated by spraying the vitamin doped water-glycerol solution on the superhydrophobic PLLA substrate.

The fabricated PLLA surface exhibited a superhydrophobic characteristic with a contact angle of 157° (**Figure 2**a and 2b). The contact angle is similar to previous reports (<154°) that

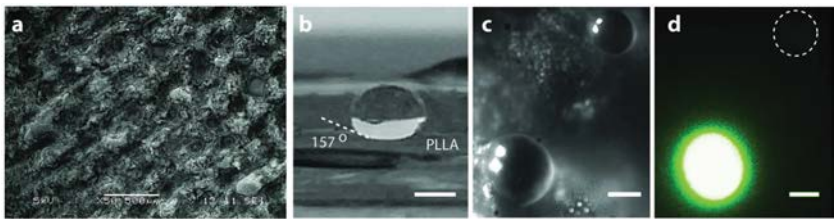

Figure 2. (a) A typical scanning electron microscopy (SEM) image of a PLLA surface generated by embossing CO_2 laser irradiated PDMS mold. (b) Water droplet on the super-hydrophobic PLLA surface. (c) Bright-field image of two vitamin microspheres on the PLLA substrate. (d) A fluorescence (pseudo-color) image of the microspheres. The one (dotted circle) placed outside the pump light did not emit fluorescence. Scale bars, 1 mm in (b) and 10 μm in (c and d).

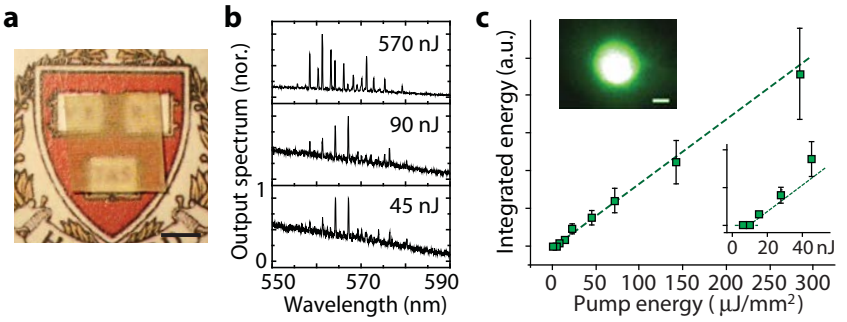

Figure 3. (a) A vitamin-polymer laser prototype. (b) Normalized emission spectra at various pump pulse energy levels. (c) Integrated energy of the laser peaks above the broad spontaneous emission background as a function of pump fluence. Line is a linear fit to data above threshold (E_{th} = 15 nJ). Error bars represent the measurement error and pulse-to-pulse variation. Upper Inset: A fluorescence (pseudo-color) micrograph of a lasing vitamin microsphere. Lower Inset: Close-up on data around the lasing threshold. Scale bars, 2.5 mm in (a) and 10 μm in (c).

have used different surface treatment methods.[23,24] For microdroplet generation, we sprayed a 1 mM FMN solution in 90% DI water and 10% glycerol with an atomizer. After the microdroplets are formed on the PLLA surface, the water evaporates, leaving the mixture of FMN and glycerol.[20] Once the water has fully evaporated, the FMN concentration in glycerol is approximately ten fold higher, resulting in a final concentration of 10 mM. The resulting droplets have a final volume in the range of 5–50 pL with diameters of 10–40 μm. Figure 2c and 2d show images of two microspheres on a PLLA substrate, in which only one of the droplets was selectively excited at low pump energy and generated fluorescence.

Figure 3a shows the first prototype with a size of 0.6 cm by 0.6 cm and a thickness of 1 mm (Figure 3a). The microspheres were formed in random locations on the surface. Upon optical pumping, we observed relatively strong spontaneous emission from the microdroplets in comparison with the previous Fabry-Perot resonator based vitamin laser. The Fabry-Perot resonator effectively filters spontaneous fluorescence emission. However, the output collected from microdroplets over a wide angle tends to contain substantial contributions from spontaneous emission. When the pump energy reached a sufficiently high level or threshold, sharp stimulated emission peaks emerged from the broad spontaneous background (Figure 3b). The number of lasing modes increased with pump energy. When pumped by 5 ns pulses at 460 nm, the typical threshold pump energy was about 15 nJ/pulse (Figure 3c). This energy corresponds to a fluence of about 10 μJ mm^{-2} and a peak intensity of 1 kW mm^{-2}. Above threshold, the integrated energy of all simultaneously lasing peaks increased linearly with pump energy (Figure 3c and Figure S4). Multi-mode lasing is commonly observed in microdroplet lasers because of spatial hole burning.[18,20,25,26] Single-mode laser emission has been observed for droplet sizes below 10 μm.[26] In our vitamin droplet laser, the lasing peaks occurred at a wavelength range between 560 and 580 nm, a small fraction of the spontaneous emission bandwidth, which further supports that the spectral peaks represent lasing modes (cf. Figure S2).[27]

Figure 4 illustrates the fabrication procedure of another microdroplet based vitamin-biopolymer laser. By using soft lithography, we first prepared a PDMS mold with a specific negative pattern that defines space to capture droplets (Figure 4a). Then, the surface roughness was tailored by surface treatment of flame brushing to make the surface hydrophobic (Figure 4b and see Methods). The PDMS mold was then used to create a PLLA film with similar surface roughness (Figure 4c,d). Finally, microdroplets of the FMN solution were formed by spraying, thus forming a spheroidal laser cavity (Figure 4e), that was then optically pumped to generate laser emission (Figure 4f). Alternatively, the microdroplets could be formed in desired microwells by using a computer controlled microdispensing system. The microdroplets in the microwells could then be further shielded by integrating a thin transparent PLLA film with a superhydrophobic-treated surface and pumped through the capping layer (Figure 4g & 4h). The encapsulation can prevent the micrdroplets from making direct contact with external environment such as tissue.

Using this technique, we fabricated a prototype (1.5 × 1.5 mm) with a patterned array of microwells (**Figure 5**a and 5b). We generated periodic micropillars with surface roughness and copied the negative pattern on the polylactic acid substrate. Each produced well has a diameter of close to 70 μm and a depth of 60 μm (Figure 5c). Then, the microdroplets are generated on the polylactic acid substrate (Figure 5d). Figure 5e

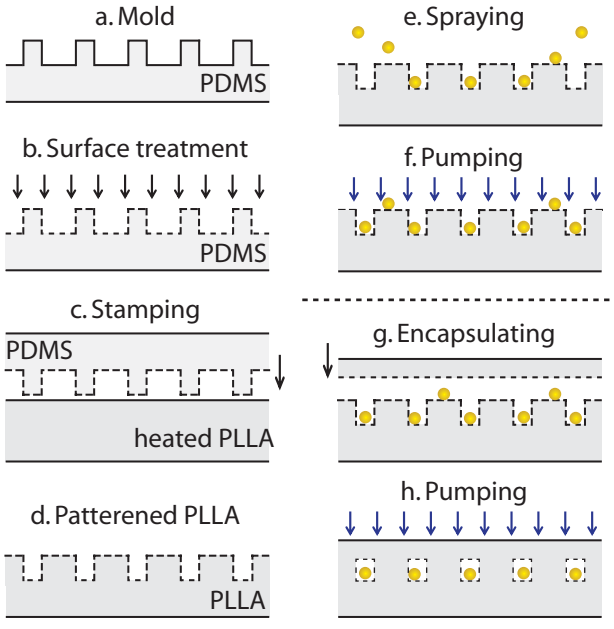

Figure 4. Illustration of the fabrication steps of a biomaterial laser using vitamin microdroplets embedded in a polymer substrate (not drawn to scale).

ADVANCED MATERIALS
www.advmat.de

www.MaterialsViews.com

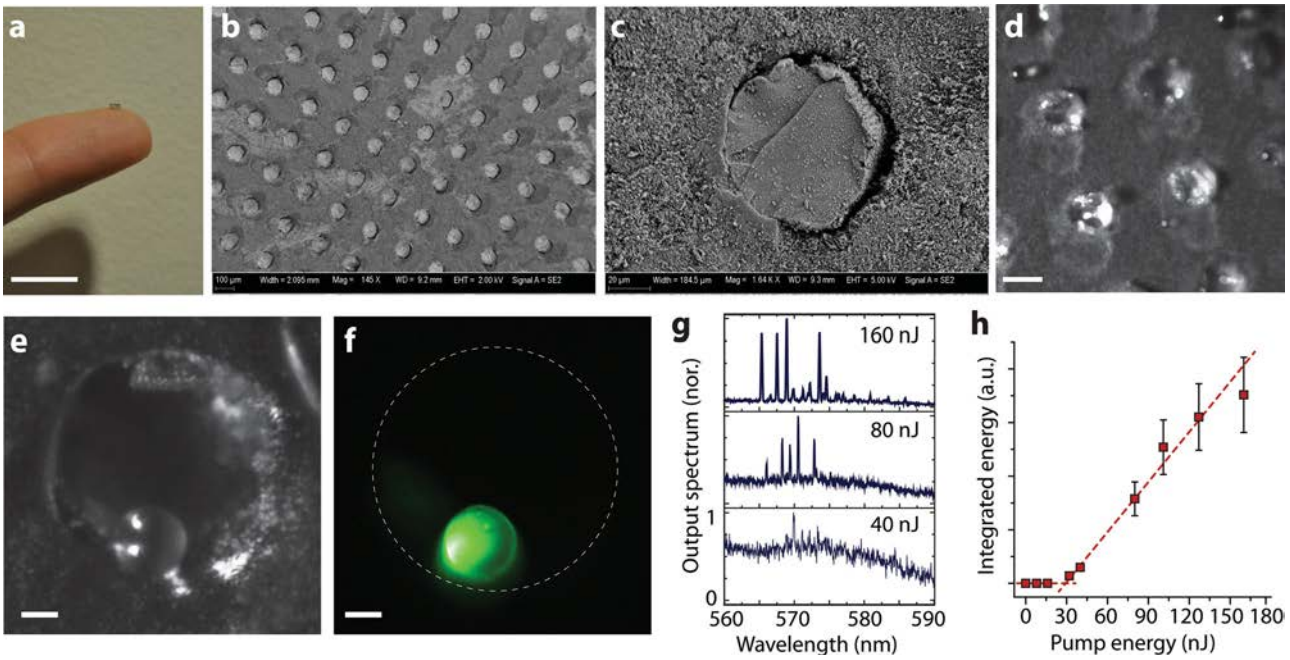

Figure 5. (a) A miniature biomaterial gain chip on a fingertip. The laser is based on vitamin microspheres embedded in PLLA microwells. (b) An SEM image of the superhydrophobic PLLA surface generated by a flame brushing technique. (c) A close-up SEM image of a single PLLA microwell. (d) A white-light micrograph of vitamin microdroplets on the PLLA substrate. (e) A brighfield image of a vitamin microsphere in a PLLA well. (f) A fluorescence (pseudo-color) image of the same microsphere above lasing threshold. (g) Normalized laser emission spectra at various pump pulse energy levels. The spectra were integrated over 0.5 s (5 pulses). Data were taken without a PLLA capping layer. (h) Integrated energy of the laser peaks as a function of pump energy. Line is a linear fit to data above threshold. Error bars represent the measurement uncertainty including pulse-to-pulse variation. Scale bars, 1 cm in (a); 200 μm in (b); 20 μm in (c); 70 μm in (d); and 10 μm in (e and f).

and f show micrographs of a single FMN microsphere formed in a microwell. Above the threshold, the lasing pulse energy increased linearly (Figure 5g) and the number of lasing modes also increased (Figure 5h). We observed an optical quality factor of the microsphere of about 3×10^3 from the spectral linewidth (0.19 nm) of the peak at 160 nJ. A non-reversible blue shift around 1.2 nm is observed in the output spectrum, which is attributed to laser induced evaporation. Assuming that the blue shift is entirely due to a reduction in droplet size, we estimate the reduction in radius to be 40 nm (assuming a perfect sphere with a diameter of 19 μm, $n_{droplet} = 1.47$ and $n_{air} = 1$).[28] Laser devices stored in normal room environment for several days showed typical lasing characteristics with similar threshold energy, which indicates the stability of microdroplets.

In conclusion, we have demonstrated an all-biomaterial laser, in which both the gain medium and the resonator-forming substrate are made of biocompatible substances. The FMN and vitamin B2 show high efficiency as the gain medium, permitting low lasing thresholds on the order of tens of nanojoules, which would not be possible by any intrinsic biomolecules in the human body. In addition, the hydrophobic surface treatment allows the formation of a microdroplet-based whispering gallery mode resonator. Our work opens up the possibility of exploring various biomaterial options and different device architectures for applications. For example, high-finesse WGM resonators and lasers have the potential for ultrahigh-sensitive sensors.[29,30] While narrowband spontaneous emission from heavy metals, such as lanthanides,[31] has shown to be advantageous for sensing, resonator-based sensing goes beyond this in terms of sensitivity because of the enhanced light-matter interaction in the cavity. By adding biosensor molecules, such as glucose-responsive monomers, such a biomaterial laser may be applied to biosensing in vivo.[32] Biocompatible optical fibers may be employed to deliver pump light to a biomaterial laser and receive signals from the sensor.

Experimental Section

Setup and measurements: Figure S1 depicts a schematic of the experimental setup for optical measurements. The pulses generated by an OPO (Quanta Ray MOPO-700, Spectra Physics; pulse duration, 5 ns, repetition rate 10 Hz, tuned to 460 nm) were reflected into the laser cavity with a dichroic mirror (500 nm, long-pass) and focused on a gain microsphere by an objective lens (with a magnification of 40X, numerical aperture of 0.95, working distance of 0.14 mm). For the mirror-based laser, an objective lens (with a magnification of 4X, numerical aperture of 0.10, working distance of 18.5 mm) instead was used. The emission from the sample was collected through the same objective and passed through the dichroic mirror. Then, the output was split with a 50/50 beam splitter to a camera that images the droplets and to a spectrometer with a cooled CCD detector (Andor) that obtains the spectrum. For the measurement of the biomaterial lasers, the spectrometer was set to 1200 grooves/mm grating and input slit width of 50 μm to have a spectral resolution of 0.04 nm. The spectra were integrated over five pulses. The laser intensity by the OPO was tuned with neutral density filters. All quoted pump energies were measured behind the microscope objective.

Fabrication of superhydrophobic surface: For the fabrication of the polylactic acid superhydrophobic surface, a two-step procedure was developed that consist of laser micromachining and molding. First, a superhydrophobic polydimethylsiloxane (PDMS) film was prepared. For this, PDMS pre-polymer was blended with a 10:1 ratio of a curing agent (Sylgard 184, Dow Corning), and the blend was mixed and de-bubbled with a smart stirrer. The uncured PDMS polymer mixture was poured on a container and cured for three hours in an oven at 65 °C. Then, the cured PDMS film was engraved with a desktop CO_2 laser machine (VersaLaser, Universal Laser System). For the engraving the power, raster speed and resolution were set approximately 1.1 W, 8 m s^{-1} and 1000 dots per inch. After the engraving the surface of the PDMS film was washed and dried to remove the residues. Afterward, the prepared PDMS surface was used as a mold to transfer the roughness to the polylactic acid surface. For this, PLLA was melted on a glass substrate at a temperature of 200 °C and the PDMS film was stamped on the PLLA surface. The film was cooled to solidify the PLLA. To fabricate microwells on PLLA, we prepared a PDMS substrate with a silicon master stamp and introduced surface roughness to make it superhydrophobic. We used a flame brushing technique, developed for inducing superhydrophobic surface of glass,[33,34] to fabricate the superhydrobphobic PDMS templates. Afterward, the negative of the structure was formed on the PLLA surface.

Measurement and calculation of contact angle: For contact angle measurement de-ionized water was used. A 4 µL droplet was placed on top of the surfaces and the image of the droplet was captured by using a home built imaging system at CNS Harvard, MET-6. Then, the captured image is processed calculated by using J-image software.[35]

Supporting Information

Supporting Information is available from the Wiley Online Library or from the author.

Acknowledgement

The authors thank Turgut Fettah Kosar for discussions on superhydrophobic surfaces and to Kyung-bok Lee for SEM images. Sedat Nizamoglu acknowledges financial support from the Bullock-Wellman Fellowship. This work was supported in part by a grant from the National Science Foundation (ECS-1101947) and by the Center for Nanoscale Systems (CNS), a member of the National Nanotechnology Infrastructure Network (NNIN), which is supported under NSF award no. ECS-0335765. CNS is part of Harvard University.

Received: February 20, 2013
Revised: May 5, 2013
Published online: July 31, 2013

[1] J. Aizenberg, A. Tkachenko, S. Weiner, L. Addadi, G. Hendler, *Nature* **2001**, *412*, 819.
[2] K. H. Jeong, J. Kim, L. P. Lee, *Science* **2006**, *312*, 557.
[3] F. G. Omenetto, D. L. Kaplan, *Science* **2010**, *329*, 528.
[4] J. G. Grote, D. E. Diggs, R. L. Nelson, J. S. Zetts, F. K. Hopkins, N. Ogata, J. A. Hagen, E. Heckman, P. P. Yaney, M. O. Stone, L. R. Dalton, *Mol. Cryst. Liquid Cryst.* **2005** *426*, 3.
[5] J. G. Grote, J. A. Hagen, J. S. Zetts, R. L. Nelson, D. E. Diggs, M. O. Stone, P. P. Yaney, E. Heckman, C. Zhang, W. H. Steier, A. K. Y. Jen, L. R. Dalton, N. Ogata, M. J. Curley, S. J. Clarson, F. K. Hopkins, *J. Phys. Chem. B* **2004** *108*, 8584.
[6] Y. Sun, S. I. Shopova, C. S. Wu, S. Arnold, X. Fan, *Proc. Natl. Acad. Sci. USA* **2010** *107*, 16039.
[7] R. H. Kim, H. Tao, T. I. Kim, Y. H. Zhang, S. Kim, B. Panilaitis, M. M. Yang, D. H. Kim, Y. H. Jung, B. H. Kim, Y. H. Li, Y. G. Huang, F. G. Omenetto, J. A. Rogers, *Small* **2012**, *8*, 2812.
[8] D. H. Kim, N. S. Lu, R. Ma, Y. S. Kim, R. H. Kim, S. D. Wang, J. Wu, S. M. Won, H. Tao, A. Islam, K. J. Yu, T. I. Kim, R. Chowdhury, M. Ying, L. Z. Xu, M. Li, H. J. Chung, H. Keum, M. McCormick, P. Liu, Y. W. Zhang, F. G. Omenetto, Y. G. Huang, T. Coleman, J. A. Rogers, *Science* **2011**, *333*, 838.
[9] A. Dupuis, N. Guo, Y. Gao, N. Godbout, S. Lacroix, C. Dubois, M. Skorobogatiy, *Opt. Lett.* **2007**, *32*, 109.
[10] S. T. Parker, P. Domachuk, J. Amsden, J. Bressner, J. A. Lewis, D. L. Kaplan, F. G. Omenetto, *Adv. Mater.* **2009**, *21*, 2411.
[11] R. Capelli, J. J. Amsden, G. Generali, S. Toffanin, V. Benfenati, M. Muccini, D. L. Kaplan, F. G. Omenetto, R. Zamboni, *Org. Electron.* **2011**, *12*, 1146.
[12] M. C. Gather, S. H. Yun, *Nature Photon.* **2011**, *5*, 406.
[13] M. C. Gather, S. H. Yun, *Opt. Lett.* **2011**, *36*, 3299.
[14] "http://www.fda.gov/Food/FoodIngredientsPackaging/GenerallyRecognizedasSafeGRAS/default.htm."
[15] P. F. Heelis, *Chem. Soc. Rev.* **1982** *11*, 15.
[16] W. Holzer, J. Shirdel, P. Zirak, A. Penzkofer, P. Hegemann, R. Deutzmann, E. Hochmuth, *Chem. Phys.* **2005**, *308*, 69.
[17] E. Cannuccia, O. Pulci, R. Del Sole, M. Cascella, *Chem. Phys.* **2011**, *389*, 35.
[18] S. X. Qian, J. B. Snow, H. M. Tzeng, R. K. Chang, *Science* **1986**, *231*, 486.
[19] M. Tona, M. Kimura, *J. Phys. Soc. Jpn.* **2000**, *69*, 3533.
[20] A. Kiraz, A. Sennaroglu, S. Doganay, M. A. Dundar, A. Kurt, H. Kalaycioglu, A. L. Demirel, *Opt. Commun.* **2007**, *276*, 145.
[21] S. Toffanin, S. Kim, S. Cavallini, M. Natali, V. Benfenati, J. J. Amsden, D. L. Kaplan, R. Zamboni, M. Muccini, F. G. Omenetto, *Appl. Phys. Lett.* **2012**, *101*, 091110.
[22] A. J. R. Lasprilla, G. A. R. Martinez, B. H. Lunelli, A. L. Jardini, R. Maciel, *Biotechnol. Adv.* **2012**, *30*, 321.
[23] W. L. Song, D. D. Veiga, C. A. Custodio, J. F. Mano, *Adv. Mat.* **2009**, *21*, 1830.
[24] N. M. Alves, J. Shi, E. Oramas, J. L. Santos, H. Tomas, J. F. Mano, *J. Biomed. Mat. Res. A* **2009**, *91A*, 480.
[25] H. B. Lin, J. D. Eversole, A. J. Campillo, *J. Opt. Soc. Am. B* **1992** *9*, 43.
[26] J. Schafer, J. P. Mondia, R. Sharma, Z. H. Lu, A. S. Susha, A. L. Rogach, L. J. Wang, *Nano Lett.* **2008** *8*, 1709.
[27] M. Humar, I. Musevic, *Opt. Express* **2011** *19*, 19836.
[28] C. C. Lam, P. T. Leung, K. Young, *J. Opt. Soc. Am. B* **1992**, *9*, 1585.
[29] E. P. Ostby, K. J. Vahala, *Opt. Lett.* **2009**, *34*, 1153.
[30] F. Vollmer, S. Arnold, *Nat. Methods.* **2008**, *5*, 591–596.
[31] A. L. Jenkins, O. M. Uy, G. M. Murray, *Anal. Chem.* **1999** *71*, 373.
[32] Y. J. Heo, H. Shibata, T. Okitsu, T. Kawanishi, S. Takeuchi, *Proc. Natl. Acad. Sci. USA* **2011**, *108*, 13399.
[33] M. Callies, D. Quere, *Soft Mat.* **2005**, *1*, 55.
[34] X. Deng, L. Mammen, H.-J. Butt, D. Vollmer, *Science* **2012**, *335*, 67.
[35] A. F. Stalder, G. Kulik, D. Sage, L. Barbieri, P. Hoffmann, *Colloid. Surface A* **2006**, *286*, 92.